Role of inertial forces on the chaotic dynamics of flexible rotating bodies

F. Calvo

Institut Lumière Matière, UMR 5306 CNRS, Université Lyon 1 and CNRS, Université de Lyon, F69622 Villeurbanne Cedex, France

(Received 5 December 2012; published 1 February 2013)

The nonlinear dynamics of isolated flexible but rotating many-body atomic systems is theoretically investigated, following the dependence on initial conditions through Lyapunov exponents. The tangent-space equations of motion that rule the time evolution of such small perturbations are rewritten in the rotating reference frame, and the various contributions of the centrifugal, Coriolis, and Euler forces are determined. Evaluating the largest Lyapunov in the rotating frame under various approximations, we show on the example of Lennard-Jones clusters that the dynamics in phase space is qualitatively at variance with the effective dynamics on the centrifugal energy surface. Coupling terms between positions and momenta in phase space, especially arising from the Coriolis force, are essential to recover the measure of chaos in the fixed reference frame.

DOI: 10.1103/PhysRevE.87.022901 PACS number(s): 05.45.Pq, 31.15.xv, 82.20.Wt, 05.45.Jn

I. INTRODUCTION

Rotation has a crucial role in the nonlinear dynamics and phase-space structures of various systems ranging from molecules [1,2] or atomic clusters [3–7] to gravity-bound systems [8], including galaxies [9]. Rotation is also essential in the development of turbulence in fluids [10], even with possible industrial implications in powder manufacturing [11]. For an isolated system, rotational motion removes some of the available energy to the expense of vibrations, which at high angular momentum usually results in the regularization of motion. However, high angular momenta can also destabilize the overall system with respect to fragmentation [12,13].

The classical dynamics of an isolated flexible many-body system conserves angular momentum in addition to total energy. The interplay between rotational and vibrational motion can be studied on the fly using projection schemes of effective or normal modes [14,15], and the kinematics in the instantaneous Eckart frame has been investigated in relation with isomerization [16]. An important advance came from Jellinek and Li [17], who identifed the effective rovibrational potential energy surface sampled by the system. This effective surface may significantly differ from the original purely vibrational energy surface, which explains how phenomena like isomerization [12,13,18–20] or fragmentation [12,13] are affected by angular momentum.

The extent of regularity or stochasticity in the dynamics is intimately connected to the local details of the potential energy surface [21], especially the curvature. In this respect it is not surprising that angular momentum affects the nonlinear dynamics, as evidenced in previous numerical simulations reporting the Lyapunov exponents [5–7]. However, in those works the effective rovibrational energy surface was not extensively involved beyond the point of providing the equilibrium geometries and the reference energy where vibrations are frozen. Although projecting onto the rotating reference frame is convenient to partition the energy into various components [15,17], it does not in itself give quantitative insight into the regularity of motion, as Lyapunov exponents are suited to.

The present work is motivated by reexamining the problem of chaotic motion of a many-body flexible system at fixed angular momentum, with the purpose of determining the Lyapunov exponent in both the fixed laboratory frame and in the rotating frame. Obviously, we do not expect differences in the calculated exponents by simply changing reference frames. However, working in the rotating reference frame allows the distinct contributions to the nonlinear dynamics to be separately identified. In particular, the roles of the centrifugal, Coriolis, and Euler inertia forces can be quantified individually.

We have applied the theory to rotating Lennard-Jones (LJ) clusters, whose nonlinear dynamics has often been investigated in the past [3–7,12–15,20–28]. Lyapunov exponents are useful quantities not only to measure the extent of chaos in the dynamics but also to provide indirect signatures of phase transitions and critical phenomena [29–32]. For such systems, the couplings between positions and momenta, which are absent in the fixed reference frame, turn out to be rather important at low energy but become negligible at high energies.

The paper is organized as follows. In the next section, we present the general tangent-space approach for a flexible system at finite angular momentum in both the fixed laboratory frame and in the rotating reference frame. We also briefly describe the way the rotating reference frame is computationally followed along the molecular dynamics trajectory. Our application to small LJ clusters is presented in Sec. III, before some discussion and conclusions are given in Sec. IV.

II. CHAOTIC DYNAMICS IN THE FIXED AND ROTATING REFERENCE FRAMES

The system of interest is made of N point particles interacting through a potential energy surface V function of the collective coordinates $\mathbf{R}_0 = \{\mathbf{r}_i^0\}$, where $\mathbf{r}_i^0$ denotes the three-dimensional position vector of particle i in the laboratory reference frame. The corresponding momenta are denoted as $\mathbf{P}_0 = \{\mathbf{p}_i^0 = m_i \dot{\mathbf{r}}_i\}$, with m_i the mass of particle i and $\dot{x}$ the time derivative of x.

For the purpose of computing the Lyapunov exponents, it is useful to introduce the notation $\varphi_0(t) = (\mathbf{R}_0, \mathbf{P}_0)$ for the set of phase-space variables. The motion of the particles follows Newton's equations, conserving the total energy E, the linear and angular momenta that are denoted as $\vec{P}$ and

$\vec{L}$, respectively. Because a finite linear momentum only alters the time evolution of the system by an extra but constant kinetic energy, we thus safely assume $\vec{P} = \vec{0}$ in what follows. These equations of motion can be written in short as the first-order equation $\dot{\varphi}_0 = F_0[\varphi_0(t)]$, where F_0 is a nonlinear multidimensional function of the positions and momenta φ_0.

A rotating reference frame can be defined by introducing the instantaneous angular velocity $\vec{\omega}(t)$ in such a way that $\vec{L} = \mathbf{I}(t) \cdot \vec{\omega}(t)$, where $\mathbf{I}(t)$ is the three-dimensional inertia tensor [17]. It should be stressed that, because the inertia tensor varies in time, so does the angular velocity vector. In this rotating frame, the coordinates and associated momenta are simply denoted as $\mathbf{R}$ and $\mathbf{P}$, respectively, or together as the variable φ. The equations of motion in the rotating frame, $\dot{\varphi} = F[\varphi(t)]$, now contain the well-known centrifugal, Coriolis, and Euler inertial terms,

$$F(\{\mathbf{r}_i;\mathbf{p}_i\}) = \begin{pmatrix} \mathbf{p}_i/\mathbf{m}_i \\ -\dfrac{\partial V}{\partial \mathbf{r}_i} + \vec{f}_i^{\,\text{centrifugal}} + \vec{f}_i^{\,\text{Coriolis}} + \vec{f}_i^{\,\text{Euler}} \end{pmatrix} \tag{1}$$

with

$$\begin{aligned} \vec{f}_i^{\,\text{centrifugal}} &= -m_i\vec{\omega} \times (\vec{\omega} \times \mathbf{r}_i) \\ \vec{f}_i^{\,\text{Coriolis}} &= -2\vec{\omega} \times \mathbf{p}_i \\ \vec{f}_i^{\,\text{Euler}} &= -m_i\dot{\vec{\omega}} \times \mathbf{r}_i. \end{aligned} \tag{2}$$

A. Tangent-space equations of motion

The Lyapunov exponents are obtained using the tangent-space method [33,34], in which a set of $6N$-dimensional vectors forming at time $t = 0$ the basis of an hypersphere monitors the distances between initially infinitesimally close trajectories. The Lyapunov exponents λ_k are obtained by the logarithmic rates of variations of the lengths ℓ_k of the axes as

$$\lambda_k = \lim_{t\to\infty} \frac{1}{t} \ln \frac{\ell_k(t)}{\ell_k(0)}. \tag{3}$$

In principle, the Lyapunov exponents do not depend on the initial point in phase space, provided that the trajectory is ergodic. For a Hamiltonian system, there are a number of zero Lyapunov exponents associated with conserved quantities, and the exponents go by positive/negative pairs [35]. The associated vectors thus can expand or shrink depending on the sign of λ_k, and it is necessary to orthonormalize the basis vectors regularly along the trajectory.

The tangent-space equations of motion describe the time variations of the initial perturbation $\delta\varphi$ of the vector φ obeying the equation $\dot{\varphi} = F(\varphi)$. Differentiation readily yields

$$\frac{d\delta\varphi}{dt} = \frac{\partial F}{\partial \varphi}\delta\varphi, \tag{4}$$

where $\partial F/\partial\varphi$ is a $6N \times 6N$ matrix referred to as the dynamical matrix. For the original equations of motion in the fixed laboratory frame, the dynamical matrix can be expressed as

$$\frac{\partial F_0}{\partial \varphi_0} = \left(\begin{array}{c|c} 0 & \begin{matrix} \ddots & \\ & 1/m_i \\ & & \ddots \end{matrix} \\ \hline -\dfrac{\partial^2 V}{\partial q_i^0 \partial q_j^0} & 0 \end{array}\right), \tag{5}$$

with $K_{ij}^0 = \partial^2 V/\partial q_i^0 \partial q_j^0$ the Hessian of the potential energy, q_i^0 being any of the $3N$ coordinates.

B. Dynamical matrix in the rotating reference frame

We now aim at calculating the dynamical matrix in the rotating frame for the phase-space vector φ rather than φ_0. Differentiating the equations of motion in the rotating frame keeps the block matrix form for $\partial F/\partial\varphi$, which we write as

$$\frac{\partial F}{\partial \varphi} = \left(\begin{array}{c|c} 0 & 1/m_i \\ \hline -K_{ij} & -C_{ij} \end{array}\right), \tag{6}$$

and where K_{ij} contains contributions from the physical and inertial forces arising from positions only, and C_{ij} are the contributions due to inertial forces that couple positions and momenta with each other. Those contributions can be explicitly written as

$$\begin{aligned} K_{ij} &= \frac{\partial^2 V}{\partial q_i \partial q_j} + K_{ij}^{\text{centrifugal}} + K_{ij}^{\text{Coriolis}} + K_{ij}^{\text{Euler}}; \\ C_{ij} &= C_{ij}^{\text{Coriolis}} + C_{ij}^{\text{Euler}}. \end{aligned} \tag{7}$$

The centrifugal force $\vec{f}_i^{\,\text{centrifugal}}$ derives from the effective centrifugal potential [17]

$$V^{\text{centrifugal}}(\mathbf{R}) = \tfrac{1}{2}\vec{\omega}^t \cdot \vec{L} = \tfrac{1}{2}\vec{L}^t \cdot \mathbf{I}^{-1} \cdot \vec{L}, \tag{8}$$

where the superscript t denotes transpose. The corresponding Hessian reads

$$\frac{\partial^2 V^{\text{centrifugal}}}{\partial q_i \partial q_j} = \frac{1}{2}\vec{L}^t \cdot \frac{\partial^2 \mathbf{I}^{-1}}{\partial q_i \partial q_j} \cdot \vec{L}, \tag{9}$$

where we have exploited the conservation of angular momentum $\vec{L}$. By differentiating $\vec{L} = \mathbf{I} \cdot \vec{\omega}$ as

$$d\vec{L} = d\mathbf{I} \cdot \vec{\omega} + \mathbf{I} \cdot d\vec{\omega} = \vec{0}, \tag{10}$$

we get

$$\frac{\partial \mathbf{I}^{-1}}{\partial q_i} = -\mathbf{I}^{-1} \cdot \frac{\partial \mathbf{I}}{\partial q_i} \cdot \mathbf{I}^{-1}, \tag{11}$$

which after further differentiating leads to

$$\begin{aligned} \frac{\partial^2 \mathbf{I}^{-1}}{\partial q_i \partial q_j} &= \mathbf{I}^{-1} \cdot \frac{\partial \mathbf{I}}{\partial q_i} \cdot \mathbf{I}^{-1} \cdot \frac{\partial \mathbf{I}}{\partial q_j} \cdot \mathbf{I}^{-1} - \mathbf{I}^{-1} \cdot \frac{\partial^2 \mathbf{I}}{\partial q_i \partial q_j} \cdot \mathbf{I}^{-1} \\ &\quad + \mathbf{I}^{-1} \cdot \frac{\partial \mathbf{I}}{\partial q_j} \cdot \mathbf{I}^{-1} \cdot \frac{\partial \mathbf{I}}{\partial q_i} \cdot \mathbf{I}^{-1}. \end{aligned} \tag{12}$$

The final expression for the centrifugal contribution can be simplified as

$$K_{ij}^{\text{centrifugal}} = \frac{1}{2}\vec{\omega}^t \cdot \left[2\frac{\partial \mathbf{I}}{\partial q_i}\cdot\mathbf{I}^{-1}\cdot\frac{\partial \mathbf{I}}{\partial q_j} - \frac{\partial^2 \mathbf{I}}{\partial q_i \partial q_j}\right]\cdot\vec{\omega}. \quad (13)$$

The contribution K_{ij}^{Coriolis} reads, in vectorial form,

$$-\frac{\partial \vec{f}_i^{\text{Coriolis}}}{\partial q_j} = 2\frac{\partial \vec{\omega}}{\partial q_j}\times \mathbf{p}_i, \quad (14)$$

which is explicit in phase-space coordinates once we express $\partial\vec{\omega}/\partial q_j$ as $-\mathbf{I}^{-1}\cdot(\partial\mathbf{I}/\partial q_j)\cdot\vec{\omega}$. Coriolis forces also produce some couplings between positions and momenta, giving some constant 3×3 block matrices

$$C_{ij}^{\text{Coriolis}} = \begin{pmatrix} 0 & -2\omega_x & 2\omega_y \\ 2\omega_x & 0 & -2\omega_z \\ -2\omega_y & 2\omega_z & 0 \end{pmatrix}. \quad (15)$$

The contribution K_{ij}^{Euler} is, again in vectorial form,

$$-\frac{\partial \vec{f}_i^{\text{Euler}}}{\partial q_j} = m_i\dot{\vec{\omega}}\times\frac{\partial \mathbf{r}_i}{\partial q_j} + m_i\frac{\partial \dot{\vec{\omega}}}{\partial q_j}\times\mathbf{r}_i. \quad (16)$$

In the above equation, the first term in the right-hand side is a simple δ function, and the only significant effort consists of evaluating $\partial\dot{\vec{\omega}}/\partial q_j$. Using again Eq. (10) we get $\dot{\vec{\omega}} = -\mathbf{I}^{-1}\cdot\dot{\mathbf{I}}\cdot\vec{\omega}$, and

$$\frac{\partial \dot{\vec{\omega}}}{\partial q_j} = \mathbf{I}^{-1}\cdot\frac{\partial \mathbf{I}}{\partial q_j}\cdot\mathbf{I}^{-1}\cdot\dot{\mathbf{I}}\cdot\vec{\omega} - \mathbf{I}^{-1}\cdot\frac{\partial \dot{\mathbf{I}}}{\partial q_j}\cdot\vec{\omega} + \mathbf{I}^{-1}\cdot\dot{\mathbf{I}}\cdot\mathbf{I}^{-1}\cdot\frac{\partial \mathbf{I}}{\partial q_j}\cdot\vec{\omega}, \quad (17)$$

in which all terms but $\mathbf{I}^{-1}$ and $\vec{\omega}$ are explicit functions of coordinates. The Euler force also contributes to some couplings between positions and momenta as

$$\frac{\partial \vec{f}_i^{\text{Euler}}}{\partial p_j} = \frac{\partial \dot{\vec{\omega}}}{\partial p_j}\times\mathbf{r}_i, \quad (18)$$

but the expression for $\partial\dot{\vec{\omega}}/\partial p_j$ can be simplified due to

$$\frac{\partial \dot{\vec{\omega}}}{\partial p_j} = -\mathbf{I}^{-1}\cdot\frac{\partial \dot{\mathbf{I}}}{\partial p_j}\cdot\vec{\omega} = -\mathbf{I}^{-1}\cdot\left(\frac{1}{m_j}\frac{\partial \mathbf{I}}{\partial q_j}\right)\cdot\vec{\omega} = -\frac{1}{m_j}\mathbf{I}^{-1}\cdot\frac{\partial \mathbf{I}}{\partial q_j}\cdot\vec{\omega} = \frac{1}{m_j}\frac{\partial \vec{\omega}}{\partial q_j}, \quad (19)$$

a term already involved in the Coriolis coupling C_{ij}^{Coriolis}.

The tangent space dynamics of the rotating system thus involves five additional terms with respect to its counterpart in the fixed laboratory frame. At this stage, the form of the dynamical matrix in Eq. (6) already suggests a few remarks. If the system is at a local minimum on the rovibrational potential energy surface, then the excess kinetic energy is stored as pure rotation with no additional vibrational energy and the terms K_{ij}^{Coriolis} and K_{ij}^{Euler} both vanish. But the coupling terms C_{ij}^{Coriolis} and C_{ij}^{Euler} do not, indicating that inertial forces will play a role on the phase-space dynamics by mixing the positions and momenta variables. This result also illustrates that the nonlinear dynamics of the rotating system cannot be partitioned as pure vibrations on the effective rovibrational surface.

However, the expressions for the various coupling additional terms are not trivial and make it difficult to evaluate their respective role, which is why we turn to a computational strategy.

C. Keeping track of the rotating frame

The numerical solution of the tangent-space equations of motion first requires the dynamics to be integrated for the main variables φ_0 of position and momenta, and this task is achieved using conventional symplectic integrators such as velocity Verlet in the fixed laboratory frame. The tangent-space equations of motion can be integrated also in this frame, providing reference data for the Lyapunov exponents.

In order to evaluate the corresponding properties in the rotating reference frame, the position and momenta φ must be determined as a function of time. In this purpose we monitor three orthonormal basis vectors $(\vec{e}_x,\vec{e}_y,\vec{e}_z)$ forming a matrix $\mathbf{E}(t)$ and that rotate with the system angular velocity $\vec{\omega}(t)$ such that $\vec{L} = \mathbf{I}\cdot\vec{\omega}$. The vectors $\vec{e}_\alpha(t)$, $\alpha = x,y,z$, are obtained also by velocity Verlet integration, from the knowledge of the first and second time derivatives given by

$$\begin{aligned} \frac{d\vec{e}}{dt} &= \vec{\omega}\times\vec{e} \\ \frac{d^2\vec{e}}{dt^2} &= \dot{\vec{\omega}}\times\vec{e} + \vec{\omega}\times(\vec{\omega}\times\vec{e}) \end{aligned} \quad (20)$$

and with $\dot{\vec{\omega}} = -\mathbf{I}^{-1}\cdot\dot{\mathbf{I}}\cdot\vec{\omega}$. The projection of positions and momenta in the laboratory frame onto the rotating frame is carried simply by matrix product with $\mathbf{E}(t)$.

III. APPLICATION TO LENNARD-JONES CLUSTERS

A. Computational details

We have calculated the largest Lyapunov exponent of two atomic clusters bound by Lennard-Jones pairwise interactions and rotating along their most stable axis. Unfortunately, it would be difficult to monitor the rotating frame for the trimer due to the possible occurrence of linear configurations and the resulting divergence of the angular velocity vector. The tetramer and icosahedral 13-mer were chosen instead. The molecular dynamics simulations were carried out at fixed total energy E and angular momentum $\vec{L}$, starting from the geometry optimized on the rovibrational potential surface $V(\mathbf{R}) + \vec{\omega}^t\cdot\vec{L}/2$. In reduced LJ units of energy (ε), distance (σ), and mass (m), the time step was taken as 10^{-2}, and the simulations consisted of 10^5 equilibration steps and 10^6 time steps over which the properties of interest were calculated. In order to prevent dissociation likely to occur at high energies, the clusters were enclosed in a soft-wall container acting on each particle i at distance r_i from the center of mass through the repulsive potential $V_{\text{rep}}(r_i) = \kappa(r_i - R)^4$ for $r_i > R$ with $\kappa = 100$ LJ units. This container is only important at high

energies and does not significantly alter the values obtained for the Lyapunov exponents. The results reported below were obtained using $R = 2$ and $R = 3$ for LJ_4 and LJ_{13}, respectively.

For the determination of the largest Lyapunov exponent based on the tangent-space method, the bred vectors $\delta\varphi_0$ and $\delta\varphi$ were initially chosen randomly with a Euclidean norm of $\|\delta\varphi\| = 10^{-10}$, and after every 100 time steps the vectors were renormalized to this value, the corresponding normalization factor contributing to the Lyapunov exponent λ. The Lyapunov exponents in the rotating frame were obtained from the exact same molecular dynamics trajectories (as resulting from specific seeds for the random generator) but by propagating the tangent-space equations for the dynamical matrix of Eq. (7) with the phase-space variables φ projected from φ_0 on the basis vector $\mathbf{E}(t)$.

B. Results

We show in Fig. 1 the variations of the largest Lyapunov exponent as a function of increasing energy in LJ_4 and LJ_{13}, for several values of angular momentum, obtained in the fixed laboratory frame and in the rotating reference frame with all terms included in the dynamical matrix of Eq. (7). In both systems, λ monotonically increases with energy but decreases with angular momentum, as the result of the increasing amount of energy stored as rotation rather than vibration. The variations are very smooth for all cases, even in the range where the clusters undergo isomerization or melting [26] and agree for LJ_{13} with previously reported results [6].

The dynamics in those two clusters thus is generally chaotic even at very low energies, indicating that the KAM threshold below which λ strictly vanishes is very low already for the tetramer, although it is known to be nonzero and measurable for the trimer [21].

The Lyapunov exponents obtained in the fixed and rotating frames essentially coincide, within minor fluctuations ascribable to uncomplete asymptotic convergence of the time average giving λ. This result was expected, because the underlying trajectory is exactly the same, only is it observed from two different reference frames. We interpret this equality as a validation of our numerical implementation of the dynamical matrix.

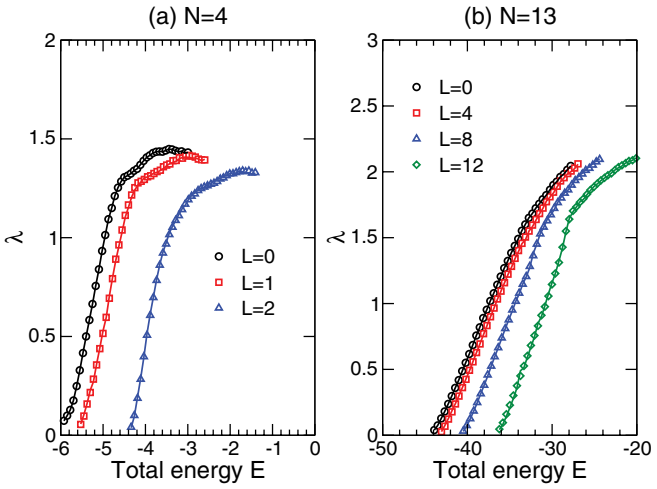

FIG. 1. (Color online) Largest Lyapunov exponent of rotating LJ_N clusters, for different values of the angular momentum L, as a function of total energy E in LJ units ε. (a) $N = 4$; (b) $N = 13$. The symbols refer to values obtained in the fixed laboratory frame, while the continuous lines show the data calculated in the rotating frame using the full dynamical matrix in Eq. (7). All quantities are expressed in reduced LJ units.

The contributions of the inertial forces to the extent of chaotic dynamics were evaluated simply by focusing on their respective roles in the dynamical matrix, neglecting the corresponding terms and reevaluating λ accordingly. We distinguish four cases, corresponding to the absence of both Coriolis and Euler forces (neglecting also the couplings between positions and momenta), the absence of either the Coriolis or Euler force (but including the appropriate couplings), and, finally, the sole neglect of coupling terms, keeping all K_{ij} terms in the dynamical matrix.

The variations of the largest Lyapunov exponent with increasing total energy are represented in Fig. 2 for the LJ tetramer with angular momenta of $L = 1$ and $L = 2$. Strikingly, the Lyapunov exponent significantly depends on the ingredients of the dynamical matrix only at low energies, and the value of λ exhibits marked changes if some of those contributions are not included.

If couplings between positions and momenta are neglected altogether, as in the case where pure centrifugal forces are considered but also when the contributions K_{ij} of the Coriolis and Euler forces are both included, the Lyapunov exponent is clearly overestimated all the more than angular momentum is high. This observation confirms our previous anticipation that coupling terms are necessarily important, because they are purely inertial and arise even for a frozen system at equilibrium on the rovibrational potential surface.

But the Coriolis and Euler forces appear to have different contributions as well. Neglecting the Euler force but keeping the Coriolis inertia is generally a rather good approximation except at very low energy. This is not a trivial result, because the Euler force is expected to become more important at high internal energy due to distortions of the principal momenta axes as anharmonic vibrations increasingly couple with rotation.

At high angular momentum, the discrepancy in the calculated λ is highest when C_{ij}^{Coriolis} is neglected, although neglecting all inertia forces except the centrifugal one achieves a more decent comparison with the reference data. It is instructive to look at the relative importance of several contributions to the dynamical matrix, and we show in Fig. 3 the variations of the modulus of the various matrices K_{ij} and of $C_{ij} = C_{ij}^{\text{Coriolis}} + C_{ij}^{\text{Euler}}$ for LJ_4 at $L = 1$, as a function of total energy. Here the modulus is defined as the average absolute value of all matrix elements. The coupling matrix remains approximately constant over the relevant energy range, at variance with the position-only contributions to the Coriolis and Euler forces that both smoothly increase. However, the Euler term increases more strongly, which reflects the increasingly large distortions of the cluster as more vibrational energy is given to the system, leading to more anharmonic variations in the inertia matrix and in the instantaneous angular velocity vector. The Euler term crosses the Coriolis term at an energy that is quite higher than the threshold at which neglecting the inertia forces in the Lyapunov

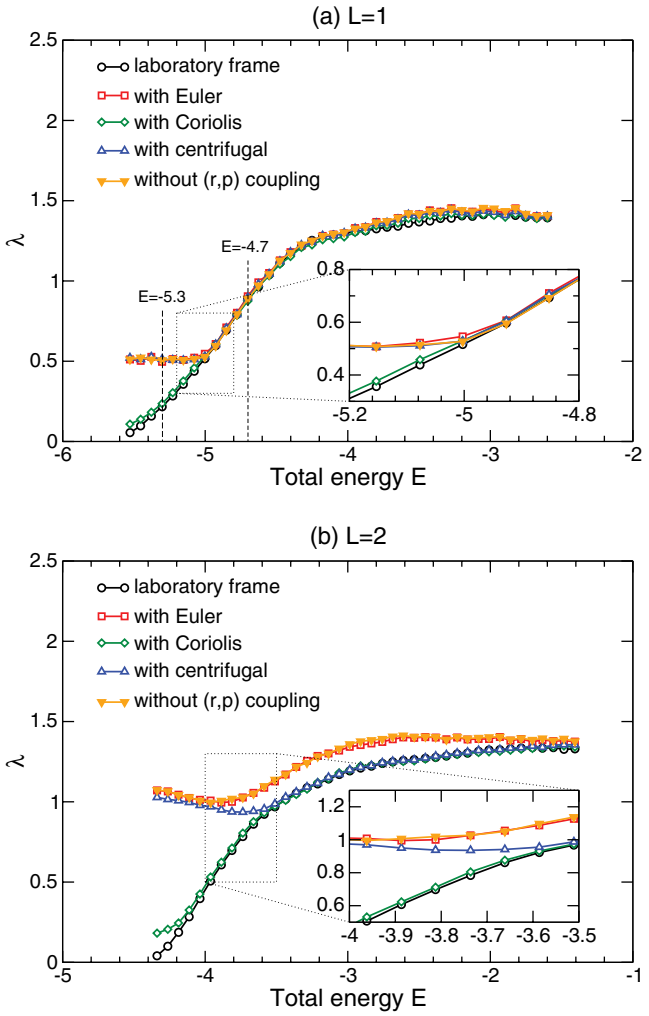

FIG. 2. (Color online) Largest Lyapunov exponent of rotating LJ_4, calculated by solving the tangent-space equations in the laboratory frame (black circles) or in the rotating frame, as a function of total energy E in LJ units ε. The results in the rotating frame are shown when considering only the centrifugal contribution (blue triangles), adding to it the Coriolis (green diamonds) or the Euler (red squares) contributions, or neglecting all couplings between positions and momenta in the dynamical matrix. (a) $L = 1$; (b) $L = 2$. In case (a), the triangle and the square symbols are practically superimposed. The regions where the various curves meet are zoomed in the insets.

calculation becomes no longer important, preventing us from attempting any tentative correlation. Unexpectedly, the least significant contribution is that of the centrifugal force, even though it is associated to changes in curvature of the potential energy surface [13].

The behavior identified on the small four-atom cluster also extends to larger systems. The variations of the largest Lyapunov exponent with internal energy are depicted in Fig. 4 at low ($L = 2$) and high ($L = 10$) angular momenta. Only three of the four approximate calculations of λ have now been considered, because the result in absence of couplings is mostly unchanged with respect to neglecting only the Euler force. For this larger system, the value of the Lyapunov exponent at high energy is again dominated by the main physical

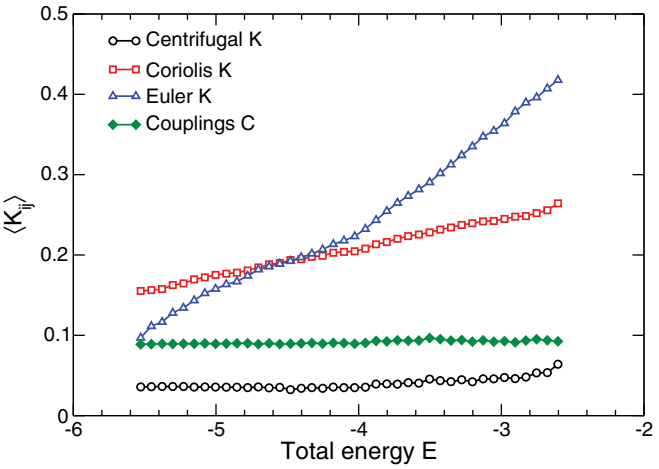

FIG. 3. (Color online) Average modulus of different contributions C_{ij} and K_{ij} to the dynamical matrix, for the LJ tetramer at $L = 1$ and as a function of increasing energy E in LJ units ε.

interactions, the inertial forces playing a negligible role. The Coriolis contribution accounts for the discrepancy in λ at low energy, and, contrary to LJ_4, no appreciable difference is found relative to the reference result of the fixed frame. The effect of angular momentum appears more clearly for this cluster, with a much higher convergence threshold energy at which the four approximations for the dynamical matrix become equally valid.

Further insight can be gained by considering the short-time (or local) Lyapunov exponents [21,23] and their statistical

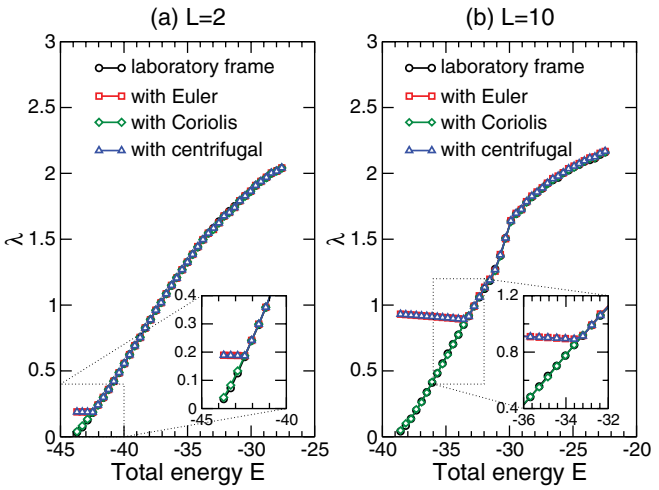

FIG. 4. (Color online) Largest Lyapunov exponent of rotating LJ_{13}, calculated by solving the tangent-space equations in the laboratory frame (black circles) or in the rotating frame, as a function of total energy E in LJ units ε. The results in the rotating frame are shown when considering only the centrifugal contribution (blue triangles) or adding to it the Coriolis (green diamonds) or the Euler (red squares) contributions. (a) $L = 2$; (b) $L = 10$. In both cases, the triangle and the square symbols are practically superimposed, and the regions where the various curves meet are zoomed in the inset.

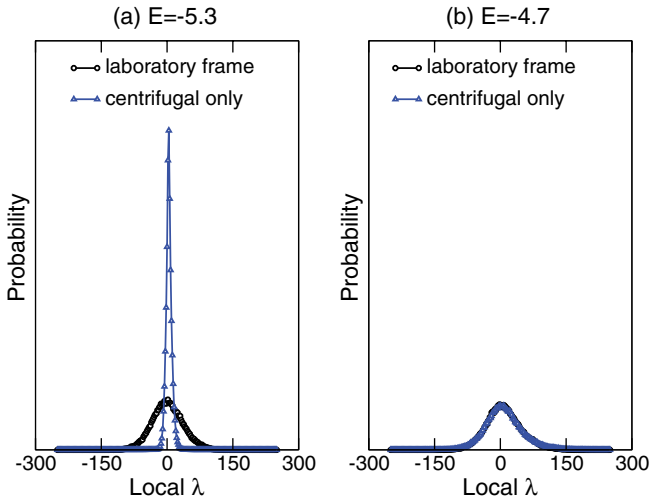

FIG. 5. (Color online) Distribution of local largest Lyapunov exponent of LJ_4 rotating at angular momentum $L = 1$, obtained in the laboratory frame (black circles) or in the rotating frame using only the centrifugal forces (blue triangles). The total energies considered are (a) $E = -5.3$; and (b) $E = -4.7$ LJ units, as highlighted in Fig. 2(a).

distributions. We have done so and show in Fig. 5 the probability of the local λ resulting from integration over only 10 time steps, for the LJ tetramer at $L = 1$ at the two total energies highlighted in Fig. 2(a) $E = -5.3$ and $E = -4.7$ LJ units, lying either below or above the convergence threshold. In the laboratory reference frame, the local Lyapunov exponent exhibits a bell shape extending more than two orders of magnitude on both sides of the average value. This extension emphasizes the necessity of performing long trajectories in order that the global exponent converges, the distributions at the two total energies being very similar and only marginally shifted with respect to each other.

The corresponding distributions obtained in the rotating reference frame on the rovibrational surface but without the Coriolis and Euler contributions are also represented in Fig 5. The distributions resulting from the neglect of either the Coriolis force or all couplings between positions and momenta, not shown, are both similar to the latter. At $E = -4.7$, consistently with the equality between the long-time exponent in Fig. 2(a), the two distributions are essentially superimposed. However, at $E = -5.3$, where the long-time exponents differ, the distribution in the rotating frame is markedly narrower and centered at a clearly higher value than its counterpart in the laboratory frame. The qualitative differences between these two distributions illustrate again the importance of momenta variables and their couplings with the positions on the Lyapunov exponents in the rotating frame.

IV. DISCUSSION AND CONCLUSIONS

Previous works on the nonlinear dynamics of rotating many-body systems have mostly emphasized the role of angular momentum on the energy partitioning and corresponding attenuation of the Lyapunov exponent [5–7]. Chaotic dynamics in nonrotating frames can be analyzed based on the local [21] or even global [36] geometric properties of the potential energy surface. At fixed angular momentum, the instantaneous rotating frame can be well defined (except maybe for systems going through a linear configuration), and the rovibrational potential surface [17] provides a convenient tool for partitioning the total energy of the system. However, in absence of other inertia forces, the particle dynamics does not faithfully account for the degree of chaoticness exhibited at low energies.

As is clearly apparent from the analysis of the dynamical matrix, couplings between positions and momenta are present even at low rovibrational energies; hence, it was not surprising that under such conditions those couplings are essential to the Lyapunov exponent in the rotating frame. This conclusion is further supported by the lower magnitude of the centrifugal part of the dynamical matrix with respect to the other inertial contributions from either the Coriolis, Euler, or coupling matrices. More surprisingly, both Coriolis and Euler forces appear to no longer contribute to the exponent above a certain energy threshold, despite the different roles played by those two forces. The results obtained for the larger cluster are robust with system size, in the sense that the inertial forces only seem to impact the regularity of the atomic motion at low energy, and this conclusion should convey to other finite systems.

The present analysis could be extended in several directions. Quantum systems could have rather different phenomenology, because angular momentum is a quantized variable and couples nontrivially with vibrations. Previous studies [25,28] have highlighted the importance of quantum effects on the chaotic behavior of nonrotating clusters, and rotation could also affect those conclusions. However, the present methodology of tangent-space dynamics would not be adapted to quantum chaos, which is best studied from the perspective of level statistics. Besides quantum effects, the entire Lyapunov spectrum of classical systems could be calculated as well to give more information about the nonlinear dynamics, with quantitative estimates of the Kolmogorov entropy. Although larger systems could be considered, it would probably be more useful to focus on the trimer, for which a wealth of computational data are available [5,7,21–23,27]. The dynamics exhibited by this small cluster is more regular as it crosses the linear saddle point [21,22,37], a feature arising due to the locally more harmonic energy surface. Also, the bimodal distribution of local Lyapunov exponents indicates that phase space is partitioned into separate sets of mixed and regular trajectories, with different corresponding time scales for ergodic convergence [23]. We expect that any finite angular momentum will also alter the dynamics at the saddle point; hence, a richer behavior is anticipated for this system. The practical difficulty amounts to determining the angular velocity as the system approaches a linear configuration. Such issues are well known in simulation [38] and could be addressed, e.g., using quaternion coordinates [39]. However, propagating the trajectory with such variables would also affect the tangent-space equations of motion, and the dynamical matrix in a rotating frame could become cumbersome [40]. This is left for future efforts.

[1] N. Fahrer and C. Schlier, J. Chem. Phys. **97**, 7008 (1992).
[2] U. Cifti and H. Waalkens, Nonlinearity **25**, 791 (2012).
[3] S. C. Farantos, J. Phys. Chem. **87**, 5061 (1983).
[4] T. L. Beck, D. M. Leitner, and R. S. Berry, J. Chem. Phys. **89**, 1681 (1988).
[5] E. Yurtsever, Europhys. Lett. **37**, 91 (1997).
[6] F. Calvo and E. Yurtsever, Phys. Lett. A **266**, 387 (2000).
[7] E. D. Belega, D. N. Trubnikov, and L. L. Lohr, Phys. Rev. A **63**, 043203 (2001).
[8] P. A. Meehan and S. F. Asckanthan, Int. J. Bifurcat. Chaos **16**, 1 (2005).
[9] P. O. Vandervoort, Mon. Not. R. Aston. Soc. **411**, 37 (2011).
[10] W. H. Finlay, J. Fluid Mech. **237**, 73 (1992).
[11] A. J. Hickey, Particul. Sci. Technol. **14**, 15 (1996).
[12] D. H. Li and J. Jellinek, Z. Phys. D: At. Mol. Clusters **12**, 177 (1989).
[13] M. A. Miller and D. J. Wales, Mol. Phys. **89**, 533 (1996).
[14] E. Yurtsever, Comput. Phys. Comm. **145**, 194 (2002).
[15] A. A. Rybakov, E. D. Belega, and D. N. Trubnikov, J. Chem. Phys. **133**, 144101 (2010).
[16] T. Yanao and K. Takatsuka, J. Chem. Phys. **120**, 8924 (2004).
[17] J. Jellinek and D. H. Li, Phys. Rev. Lett. **62**, 241 (1989).
[18] L. L. Lohr, Int. J. Quantum Chem. **57**, 707 (1996).
[19] L. L. Lohr, Mol. Phys. **97**, 977 (1999).
[20] E. Yurtsever, Phys. Rev. E **63**, 016202 (2000).
[21] D. J. Wales and R. S. Berry, J. Phys. B **24**, L351 (1991).
[22] R. J. Hinde, R. S. Berry, and D. J. Wales, J. Chem. Phys. **96**, 1376 (1992).
[23] C. Amitrano and R. S. Berry, Phys. Rev. Lett. **68**, 729 (1992).
[24] V. Mehra and R. Ramaswamy, Phys. Rev. E **56**, 2508 (1997).
[25] C. Chakravarty, R. J. Hinde, D. M. Leitner, and D. J. Wales, Phys. Rev. E **56**, 363 (1997).
[26] F. Calvo, J. Chem. Phys. **108**, 6861 (1998).
[27] J. R. Green, J. Jellinek, and R. S. Berry, Phys. Rev. E **80**, 066205 (2009).
[28] F. Calvo, Physica D **240**, 1001 (2011).
[29] P. Butera and G. Caravati, Phys. Rev. A **36**, 962 (1987).
[30] A. Bonasera, V. Latora, and A. Rapisarda, Phys. Rev. Lett. **75**, 3434 (1995).
[31] V. Latora, A. Rapisarda, and S. Ruffo, Phys. Rev. Lett. **80**, 692 (1998).
[32] F. Ginelli, K. A. Takeuchi, H. Chaté, A. Politi, and A. Torcini, Phys. Rev. E **84**, 066211 (2011).
[33] I. Shimada and T. Nagashima, Prog. Theor. Phys. **61**, 1605 (1979).
[34] G. Benettin, L. Galgani, A. Giorgilli, and J.-M. Strelcyn, Meccanica **15**, 9 (1980).
[35] H.-D. Meyer, J. Chem. Phys. **84**, 3147 (1986).
[36] L. Casetti, C. Clementi, and M. Pettini, Phys. Rev. E **54**, 5969 (1996).
[37] T. Komatsuzaki and R. S. Berry, Proc. Natl. Acad. Sci. USA **98**, 7666 (2001).
[38] M. P. Allen and D. J. Tildesley, *Computer Simulations of Liquids* (Oxford University Press, Oxford, 1987).
[39] D. J. Evans, Mol. Phys. **34**, 317 (1977).
[40] F. Calvo, Phys. Rev. E **58**, 5643 (1998); **60**, 2771 (1999).